Analysis of time delay effects on a linear bubble chain system[a)]

Andrew Ooi[b)] and Aneta Nikolovska[c)]
Department of Mechanical Engineering, The University of Melbourne, Parkville Melbourne, Victoria 3010, Australia

Richard Manasseh[d)]
Fluid Dynamics Group, CSIRO Manufacturing Science and Engineering, P.O. Box 56 (Graham Road), Highett, Melbourne, Victoria 3190, Australia

(Received 30 July 2007; revised 16 May 2008; accepted 19 May 2008)

A chain of vertically rising discrete air bubbles represents a transition phenomenon from individual to continuum behavior in a bubbly liquid. Previous studies have reported that there is a preference for acoustic energy to propagate along the bubble chain and that this behavior could be explained by a coupled-oscillator model. However, it has recently been demonstrated that quantitative results from the coupled-oscillator model do not match experimental data. In this paper, it is shown how adding time delays to the coupled-oscillator model can produce results that are in better agreement with experimental data. In addition, the effects of time delays on the natural frequencies and damping of individual eigenmodes of the vertical bubble chain are also investigated. It was found that adding time delays can dramatically change the damping of the different modes of the system while having less dramatic impact on the natural frequencies of the individual eigenmodes. Counterintuitively, it is found that the effects of time delays appear to be more important when the bubbles are closer together than when they are farther apart. © *2008 Acoustical Society of America.* [DOI: 10.1121/1.2945156]

PACS number(s): 43.30.Nb, 43.20.Fn, 43.20.Px, 43.20.Bi [RCG] Pages: 815–826

I. INTRODUCTION

Many researchers have directed efforts towards the development of a model to describe the volumetric oscillations of gas bubbles in liquid. The acoustic behavior of an isolated bubble has been extensively researched (see Ref. 1 and references therein). There have also been many publications on the dynamics of the acoustic field in the vicinity of bubble pairs (see Refs. 2–9). More recently, Ida[10] has extended this line of investigation and studied the natural frequencies of a system consisting of three bubbles of different sizes. When there are many bubbles in the medium, Commander and Prosperetti,[11] Duraiswami *et al.*,[12] and Nicholas *et al.*[13] have taken the continuum approach and have assumed a spatially homogeneous medium with the void fraction being the important parameter. These continuum theories have been used by Phelps *et al.*,[14] Duraiswami *et al.*,[12] and Terrill and Melville[15] as the basis of several instruments for oceanographic and industrial applications. Most of these systems measure bubble-size distributions, relying on an active principle. Sound is sent into the water and the attenuation or reflection of the resulting signal is interpreted to infer the bubble-size distribution. On the other hand, there are passive systems, which rely on bubbles emitting sound at their natural frequencies. It is not difficult to obtain experimental pressure signals emitted (passively) by a bubbly flow and such measurements have been made for many years (see Refs. 15–18). However, most analyses have been carried out in the frequency domain, with attention focusing on how to convert the spectra into bubble-size distributions. Above all, most analyses assume the bubbles are isotropically and homogeneously distributed in the fluid, which is, in fact, a rarity, either in nature or industry.

The acoustic signature of a finite number of discrete air bubbles represents an important yet little-researched area in multiphase flow. The scattering of acoustic waves from gas bubbles in liquids plays a crucial role in determining the acoustic attenuation and dissipation in the surrounding medium. Such systems could provide insight into sound propagation in the anisotropic and inhomogeneously distributed bubbly systems that are the norm in practice. The current work is aimed at the analysis of the coupled-oscillator mathematical model when applied to a vertical chain of bubbles (for example, see Fig. 1) in which the individual bubbles resonate in the monopole (isotropic) mode (see Ref. 19). Even though the propagation of acoustic energy generated by each individual bubble might be isotropic, it has been found that the distribution of acoustic energy close to a bubble chain is not isotropic, due to the interaction of the acoustic waves with other bubbles. Manasseh *et al.*[20] and Nikolovska *et al.*[21] have applied a coupled-oscillator formalism to describe the collective scattering due to multiple gas bubbles in a chain. The sound was initiated naturally on the detachment of each bubble from a nozzle at the base of the chain and the effects of other bubbles were modeled through a set of coupled ordinary differential equations.

[a)]Submitted in August 2007 to the Journal of the Acoustical Society of America.
[b)]Electronic mail: a.ooi@unimelb.edu.au
[c)]Electronic mail: aneta@uni-bremen.de
[d)]Electronic mail: richard.manasseh@csiro.au

FIG. 1. (Color online) Photo of a typical bubble chain.

In this paper, an analysis is carried out using the coupled-oscillator model proposed by Feuillade[6] and used by many others (Feuillade,[19] Tolstoy,[3] and Doinikov *et al.*[22]). In particular, the effects of time delays on the natural frequencies and damping of the bubble chain system will be highlighted. A time delay arises from the finite speed of sound propagation in the liquid or, in other words, from the finite compressibility of the liquid. As a result, the acoustic pressure field influencing the oscillations of all the other bubbles is a time-retarded field.[22] The present work is essentially an extension of the study carried out by Doinikov *et al.*,[22] which highlighted the effects of time delays on a bubble chain with different numbers of bubbles. In Ref. 22, the effects of adding more bubbles in the chain were investigated. The distance between the bubbles was kept constant so when more bubbles were added into the system, the bubble chain just became longer. This is very different to what happens in laboratory experiments, where it is more common for the length of the bubble chain to be kept constant because the water tank used is likely to be of a constant height. The number of bubbles in the chain can be increased by increasing the airflow rate in the nozzle and as a result, the distance between the bubbles in the chain will also become smaller. Hence, the distance between the bubbles is an important parameter in the problem and the effects of time delays as a function of bubble separation are investigated in the present paper.

II. GOVERNING EQUATIONS AND ANALYSIS

In the following analysis, the "self-consistent" approach (see previous work by Tolstoy,[3] Feuillade,[19] and Feuillade[6]) will be used. This is one method of overcoming (or rather side-stepping) the problem of infinite rereflexions in coupled multibubble systems. The total pressure field incident on any bubble is taken as the sum of the pressure fields radiated by all the other bubbles in the system, plus any external forcing. However, acoustic energy emitted by a bubble, once incident on a second bubble, is reradiated back to the first, and so on, creating an infinite series, analogous to a pair of mirrors facing each other. With many bubbles, this is analytically problematic. This problem arises in many scattering phenomena in physics, not only in acoustics.[3] The key to the self-consistent approach is that the pressure fields from the other bubbles are defined to have already experienced the infinity of other interactions, which affect them. One consequence is that the dependent variables [which will be defined as $x_n(t)$ below] lose their precise physical meaning as the radial perturbation of the nth bubble. The merits of using the self-consistent approach as opposed to the alternative multiple scattering approach have been discussed by Feuillade[6] and Twersky.[23]

In order to simplify the analysis, it will also be assumed that the equilibrium radii of all bubbles in the chain are the same and that the distance between the neighboring bubbles in the chain is constant. In the experiments, the bubble rise velocity was higher further up the chain[20] owing to the initial acceleration of the bubbles from their detachment point at the base of the chain. Hence, the spacing between the bubbles was larger higher up the bubble chain.

As the effort in this paper is to extend the work presented by Doinikov *et al.*,[22] the same notation as in that paper will be used. Using the assumptions above and assuming a compressible liquid (i.e., a finite speed of sound propagation), small, radial free oscillations of N coupled bubbles are described by the following equations:

$$\ddot{x}_n(t) + \omega_0 \delta \dot{x}_n(t) + \omega_0^2 x_n(t) = -\sum_{m=1, m\neq n}^{N} \frac{R_0}{d_{nm}} \ddot{x}_m(t - d_{nm}/c), \tag{1}$$

where, in the absence of radiative interactions, $x_n(t)$ is the (small) change in radius of the nth bubble. Because we use the self-consistent approach, x_n is defined to include the effects of radiative interactions in the system and hence can no longer be precisely compared with the behavior of the nth bubble. However, for the present paper, that is not a problem since comparisons with experiment are only being made with quantities such as pressure and propagation speed, not on the

behavior of individual bubbles. R_0 is the equilibrium radius, d_{nm} is the distance between the centers of the nth and mth bubbles, and c is the speed of sound in bubble-free water. δ is the total damping coefficient of an isolated bubble consisting of radiation and thermal and viscous dampings (see Refs. 1 and 24). We assume adiabatic conditions and the resonant (Minnaert) angular frequency is calculated as

$$\omega_0 = \frac{1}{R_0}\sqrt{\frac{3\gamma p_0}{\rho}},$$

where p_0 is the static pressure, $\gamma = 1.4$ is the ratio of specific heats, and ρ is the density of the liquid. The coupling term on the right hand side of Eq. (1) is the time delay term and it reflects the finite time it takes for a disturbance to reach a nearby bubble. For an incompressible fluid, $c = \infty$, hence Eq. (1) can be simplified to

$$\ddot{x}_n(t) + \omega_0 \delta \dot{x}_n(t) + \omega_0^2 x_n(t) = -\sum_{m=1, m\neq n}^{N} \frac{R_0}{d_{nm}} \ddot{x}_m(t). \tag{2}$$

It must be noted that Eqs. (1) and (2) assume that the acoustic field that affects a bubble is predominantly from a monopolar source (see Ref. 6). This suggests that Eqs. (1) and (2) should only be used in situations where $d_{nm} \gg R_0$ (see Ref. 22).

The solution to Eqs. (1) and (2) can be expressed in the form

$$\mathbf{x}(t) = \mathbf{A}e^{\lambda t}, \tag{3}$$

where $\mathbf{x}(t)$ is a vector whose individual components are $x_n(t)$ and $\mathbf{A}$ is the eigenvector corresponding to the eigenvalue λ. Substituting Eq. (3) into Eq. (1) gives

$$[\lambda^2 \mathbf{I} + \lambda \mathbf{C} + \mathbf{K}]\mathbf{A} = -\lambda^2 \mathbf{R}(\lambda)\mathbf{A}, \tag{4}$$

where $\mathbf{I}$ is the identity matrix,

$$\mathbf{C} = \omega_0 \delta \mathbf{I},$$

$$\mathbf{K} = \omega_0^2 \mathbf{I},$$

and

$$\mathbf{R} = \begin{bmatrix} 0 & (R_0/d_{12})e^{-\lambda\tau_{12}} & (R_0/d_{13})e^{-\lambda\tau_{13}} & \cdots & \cdots & (R_0/d_{1N})e^{-\lambda\tau_{1N}} \\ (R_0/d_{21})e^{-\lambda\tau_{21}} & 0 & (R_0/d_{23})e^{-\lambda\tau_{23}} & \cdots & \cdots & (R_0/d_{2N})e^{-\lambda\tau_{2N}} \\ (R_0/d_{31})e^{-\lambda\tau_{31}} & \cdots & 0 & (R_0/d_{34})e^{-\lambda\tau_{34}} & \cdots & (R_0/d_{3N})e^{-\lambda\tau_{3N}} \\ (R_0/d_{41})e^{-\lambda\tau_{41}} & \cdots & \cdots & 0 & \cdots & (R_0/d_{4N})e^{-\lambda\tau_{4N}} \\ \vdots & \cdots & \cdots & \cdots & 0 & \vdots \\ (R_0/d_{N1})e^{-\lambda\tau_{N1}} & \cdots & \cdots & \cdots & \cdots & 0 \end{bmatrix}.$$

$\mathbf{R}(\lambda)$ is a symmetric matrix with zeros along the main diagonal. The off-diagonal terms are exponential functions of $\lambda\tau_{nm}$, where $\tau_{nm} = d_{nm}/c$ is the time delay. It is more conventional to write Eq. (4) as

$$\mathbf{D}(\lambda, \tau_{nm}) = [\lambda^2(\mathbf{I} + \mathbf{R}(\lambda)) + \lambda\mathbf{C} + \mathbf{K}]\mathbf{A} = \mathbf{0}. \tag{5}$$

Equation (5) represents a nonlinear eigenvalue problem. Given values of τ_{nm}, one needs to find values of λ (eigenvalues) such that the determinant of $\mathbf{D}$ is zero. For a $N \times N$ system, there are $2N$ eigenvalues,

$$\lambda = \xi \pm i\omega, \tag{6}$$

where ω is the natural frequency, ξ is the damping for the particular eigenvector (mode), and i is the imaginary unit. The eigenvalues occur in complex conjugate pairs.

For a bubble in isolation, it can easily be shown that

$$\lambda = -\frac{\omega_0 \delta}{2} \pm i\omega_0 \sqrt{\left(1 - \frac{\delta^2}{4}\right)}.$$

thus,

$$\xi_0 = \frac{\omega_0 \delta}{2}$$

and

$$\omega_{01} = \omega_0 \sqrt{\left(1 - \frac{\delta^2}{4}\right)}.$$

Note that for the millimeter-sized bubbles considered in this paper, δ is small so $\omega_{01} \approx \omega_0$. In the presentation of results below, all data will be normalized with the parameters from the isolated bubble case, i.e.,

$$\xi^* = \frac{\xi}{\xi_0} \quad \text{and} \quad \omega^* = f^* = \frac{\omega}{\omega_{01}}. \tag{7}$$

If time delays are neglected (i.e., if the liquid is assumed to be incompressible), then $\tau_{nm} = 0$ and the matrix $\mathbf{I} + \mathbf{R}$ in Eq. (5) no longer consists of any exponential functions. Hence, we have a conventional quadratic eigenvalue problem. This type of problem has many applications and has been studied extensively by many researchers (see Ref. 25 and references therein). The eigenvalues and eigenvectors for the quadratic eigenvalue problem can be obtained using standard numeri-

cal routines that are widely available (e.g., the *polyeig* function in MATLAB 7.0). If time delays are taken into consideration, then obtaining the eigenvectors and eigenvalues of Eq. (5) is more complicated. A method of finding the eigenvalues for time delay systems has been outlined by Hu *et al.*[26] In that paper, they introduced a numerical method to obtain eigenvectors and eigenvalues for a system where there is time delay in x and $\dot{x}$ in the governing equation. Furthermore, Hu *et al.*[26] only considered systems where there is only one (constant) time delay for the whole system. Thus, the system considered here is different to the problems considered by Hu *et al.*[26] in two respects. Firstly, the time delay is in the $\ddot{x}$ term [see Eq. (1)], and secondly, the time delays, τ_{nm}, are not constants but are dependent on the distance between bubbles n and m. Hence, the method suggested by Hu *et al.*[26] needs to be modified and extended for the system of equations that is of interest here.

First, consider the case where time delays are neglected, i.e., $\tau_{nm}=0$. We require a solution for $\mathbf{A}_r$ and λ_r that satisfies

$$\mathbf{D}(\lambda_r,0)\mathbf{A}_r = 0. \tag{8}$$

This represents a conventional quadratic eigenvalue problem. When one takes into account time delays, then there exists an eigenvalue, λ_t, and eigenvector, $\mathbf{A}_t$, near λ_r and $\mathbf{A}_r$ such that the following condition is true:

$$\mathbf{D}(\lambda_t,\tau_{nm})\mathbf{A}_t = 0, \tag{9}$$

i.e., λ_t and $\mathbf{A}_t$ are the eigenvalues and eigenvectors of the time delay system [Eq. (9)]. We will write

$$\lambda_t = \lambda_r + \Delta\lambda_r \quad \text{and} \quad \mathbf{A}_t = \mathbf{A}_r + \Delta\mathbf{A}_r. \tag{10}$$

Substituting Eq. (10) into Eq. (9) gives

$$\mathbf{D}(\lambda_r + \Delta\lambda_r, \tau_{nm})(\mathbf{A}_r + \Delta\mathbf{A}_r) = 0. \tag{11}$$

If we perform a Taylor series expansion about λ_r and ignore terms of the order of $(\Delta\lambda_r)^2$ and $\Delta\lambda_r\Delta A_r$, then one may write

$$\mathbf{D}(\lambda_r,\tau_{nm})(\mathbf{A}_r + \Delta\mathbf{A}_r) = \Delta\lambda_r\mathbf{E}(\lambda_r,\tau_{nm})(\mathbf{A}_r), \tag{12}$$

where

$$\mathbf{E}(\lambda_r,\tau_{nm}) = -(2\lambda_r\mathbf{I} + \mathbf{R}(-\lambda_r^2\tau_{nm} + 2\lambda_r) + \mathbf{C}). \tag{13}$$

Following Hu *et al.*,[26] we define a vector $\mathbf{P}_r$ such that

$$\mathbf{P}_r = \frac{1}{\Delta\lambda_r}(\mathbf{A}_r + \Delta\mathbf{A}_r). \tag{14}$$

Equation (12) can now be written as

$$\mathbf{D}(\lambda_r,\tau_{nm})\mathbf{P}_r = \mathbf{E}(\lambda_r,\tau_{nm})\mathbf{A}_r. \tag{15}$$

In order to solve Eq. (15), consider the ratio

$$\frac{\mathbf{P}_r^*\mathbf{D}(\lambda_r,\tau_{nm})\mathbf{P}_r}{\mathbf{P}_r^*\mathbf{E}(\lambda_r,\tau_{nm})\mathbf{P}_r} = \frac{\mathbf{P}_r^*\mathbf{E}(\lambda_r,\tau_{nm})\mathbf{A}_r}{\mathbf{P}_r^*\mathbf{E}(\lambda_r,\tau_{nm})\mathbf{P}_r}, \tag{16}$$

where $\mathbf{P}_r^*$ is the complex conjugate of $\mathbf{P}_r$. However, $\mathbf{P}_r$ and $\mathbf{A}_r$ are related to Eq. (14), so Eq. (16) can be written as

$$\begin{aligned}\frac{\mathbf{P}_r^*\mathbf{D}(\lambda_r,\tau_{nm})\mathbf{P}_r}{\mathbf{P}_r^*\mathbf{E}(\lambda_r,\tau_{nm})\mathbf{P}_r} &= \frac{\mathbf{P}_r^*\mathbf{E}(\lambda_r,\tau_{nm})\mathbf{A}_r}{\mathbf{P}_r^*\mathbf{E}(\lambda_r,\tau_{nm})(\mathbf{A}_r+\Delta\mathbf{A}_r)/\Delta\lambda_r} \\ &= \Delta\lambda_r\frac{\mathbf{P}_r^*\mathbf{E}(\lambda_r,\tau_{nm})\mathbf{A}_r}{\mathbf{P}_r^*\mathbf{E}(\lambda_r,\tau_{nm})(\mathbf{A}_r+\Delta\mathbf{A}_r)} \\ &= \Delta\lambda_r\frac{\mathbf{P}_r^*\mathbf{E}(\lambda_r,\tau_{nm})\mathbf{A}_r}{\mathbf{P}_r^*\mathbf{E}(\lambda_r,\tau_{nm})\mathbf{A}_r + \mathbf{P}_r^*\mathbf{E}(\lambda_r,\tau_{nm})\Delta\mathbf{A}_r} \\ &= \Delta\lambda_r\left(1 - \frac{\mathbf{P}_r^*\mathbf{E}(\lambda_r,\tau_{nm})\Delta\mathbf{A}_r}{P_r^*\mathbf{E}(\lambda_r,\tau_{nm})\mathbf{A}_r} + \cdots\right).\end{aligned} \tag{17}$$

Hence, $\Delta\lambda_r$ can be approximated as

$$\Delta\lambda_r \approx \frac{\mathbf{P}_r^*\mathbf{D}(\lambda_r,\tau_{nm})\mathbf{P}_r}{\mathbf{P}_r^*\mathbf{E}(\lambda_r,\tau_{nm})\mathbf{P}_r}. \tag{18}$$

So the eigenvalues, λ_t, and eigenvectors, $\mathbf{A}_t$, for the time delay problem can be calculated as follows.

(1) Obtain the eigenvalues, λ_r, and eigenvectors, $\mathbf{A}_r$, assuming that time delays $\tau_{nm}=0$. This can be done using standard techniques described in Ref. 25.
(2) λ_r and $\mathbf{A}_r$ are good initial guesses for the eigenvalues and eigenvectors of the system with time delay. We let $\lambda_t'=\lambda_r$ and $\mathbf{A}_t'=\mathbf{A}_r$, where λ_t' and $\mathbf{A}_t'$ are the initial guesses for λ_t and $\mathbf{A}_t$.
(3) Construct the matrix $\mathbf{E}(\lambda_t', \tau_{nm})$ [see Eq. (13)] from λ_t'.
(4) Solve Eq. (15) to obtain P_r.
(5) Use Eq. (18) to obtain an estimate for $\Delta\lambda_r$. The new value for λ_t' can now be calculated to be $\lambda_r+\Delta\lambda_r$.
(6) Use Eq. (14) to calculate a new estimate for the eigenvector $\mathbf{A}_t'=\mathbf{A}_r+\Delta\mathbf{A}_r$.
(7) Go back to step 3 with the new values of λ_t' and $\mathbf{A}_t'$ until the values of λ_t' and $\mathbf{A}_t'$ do not change anymore. Once the solution is converged, $\lambda_t=\lambda_t'$ and $\mathbf{A}_t=\mathbf{A}_t'$.

From our numerical calculations, it was found that, in general, for small values of D/R_0, where D is the spacing between the centers of two adjacent bubbles, the eigenvalues of the time delay system occur in distinct complex conjugate pairs for small values of N. For larger values of N, the eigenvalues move closer together. Sometimes, in the numerical iterations, it is possible to converge to the same eigenvalue even though different starting guesses were used. To overcome this problem, the eigenvectors and eigenvalues are first obtained with small values of D (only in the time delay term). Then, these eigenvalues and eigenvectors are used as guesses for the system with the desired value of D.

Once the eigenvalues and eigenvectors of the time delay system are obtained, the solution in the physical domain can be constructed by a linear combination of $\mathbf{A}_r$ and corresponding λ_r,

$$\mathbf{x}(t) = \sum_{n=1}^{N} \beta_n\mathbf{A}_{n,t}e^{\lambda_{n,t}t}, \tag{19}$$

where β_n are constants to be determined from the initial conditions.[19] At time $t=0$, it will be assumed that

$$\mathbf{x}(t=0) = \begin{Bmatrix} 1 \\ 0 \\ 0 \\ 0 \\ \vdots \\ 0 \end{Bmatrix}. \tag{20}$$

It will also be assumed that

$$\frac{d\mathbf{x}}{dt}(t=0) = \mathbf{0}.$$

This is only for the sake of convenience because it is not known what values to use at $t=0$. The correct values to use for $d\mathbf{x}/dt(t=0)$ and $\mathbf{x}(t=0)$ require extensive studies of the bubble wall oscillations as the bubble is formed and initially perturbed. Neither experimental nor numerical data on the magnitudes of these naturally initiated oscillations are easy to obtain; this is a subject of active research (see, for example, Refs. 27–31) that is beyond the scope of the current manuscript.

III. RESULTS AND DISCUSSION

The results will be divided into two sections. Section III A investigates the effects of adding time delays to the mathematical model. The bubbles that were considered had a radius of 2 mm, since millimeter-sized bubbles are usually excited only to the small amplitudes for which the linear theory presented above is valid. Results from simulations carried out using the model both with and without time delays are presented in Sec. III B. The theoretical data are compared with experimental data in order to ascertain if time delays are needed in order to better represent the physics of the problem.

A. Analysis of the eigenvalues

As a reference, it would be instructive to first compare the effects of time delay for the case when there are just two bubbles in the chain. For this case, the higher order $n=2$ mode corresponds to the case when the bubbles oscillate 180° out of phase with each other. The $n=1$ mode corresponds to the situation when the two bubbles oscillate in phase with each other. Figure 2 shows the damping and frequency plots if time delays are not taken into account. The distance, D, between the two bubbles is normalized by $\lambda = c/f_0$, which is the wavelength associated with the natural frequency $f_0 = \omega_0/(2\pi)$ of an isolated bubble. The calculated mode damping, ξ, and frequency, f, are normalized according to Eq. (7).

As can be seen, the highest frequency ($n=2$) mode has the highest values of damping as is found in many natural oscillatory systems. An extension of this work to investigate how the natural frequencies of a bubble system change in the presence of a wall have been reported by Payne *et al.*[32] It is also interesting to note that there is no crossing over of the frequency and the damping, i.e., for all values of D, the $n=2$ mode always has a higher frequency and damping than the $n=1$ mode. When the time delay is taken into consideration, the results are shown in Fig. 3. There are clear differences with the information shown in Fig. 2. Most obviously, the curves for the $n=1$ and the $n=2$ modes cross over at distinct values of D/λ. The $n=1$ and $n=2$ curves for ξ^* cross over at $D/\lambda=(k+1)/2$ where $k=0,1,2,\ldots$, and the curves for f^* cross over when $D/\lambda=(2k+1)/4$ where $k=0,1,2,\ldots$. When the bubbles are close together [i.e., when $D/\lambda < (1/4)$], the damping for the $n=1$ mode is greater than the damping of the $n=2$ mode but the natural frequency for the $n=2$ mode is greater than the $n=1$ mode. This is in stark contrast to the results when the time delay is not taken into account. When $(1/4) < D/\lambda < (2/4)$, there is a crossing over of the natural frequencies to create a situation where the $n=1$ mode has a higher frequency than the $n=2$ mode and the damping of the $n=1$ mode is still higher than the $n=2$ mode.

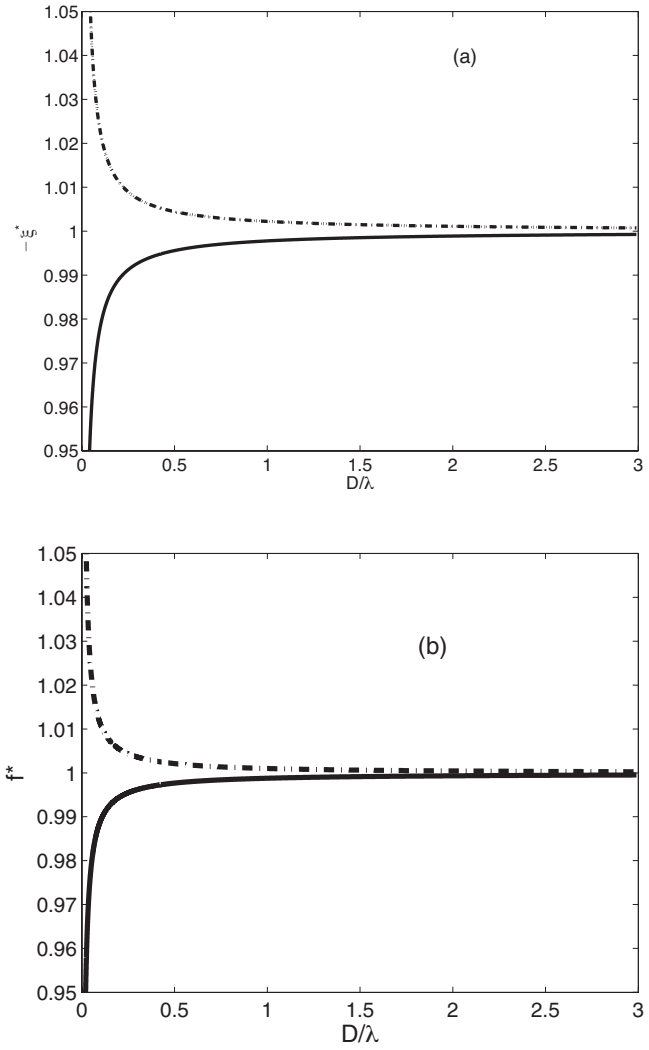

FIG. 2. Plot of $-\xi^*$ (a) and f^* (b) for the different modes predicted by the model without time delay. (—) $n=1$; (–·–) $n=2$. There are only two bubbles in the system and $R_0=2$ mm.

To understand the effects of time delay on the damping of a two-bubble system, consider the following coupled set of delay differential equations:

$$\ddot{x}_1(t) + \omega_0 \delta \dot{x}_1(t) + \omega_0^2 x_1(t) = -\frac{R_0}{D}\ddot{x}_2(t-\tau), \tag{21}$$

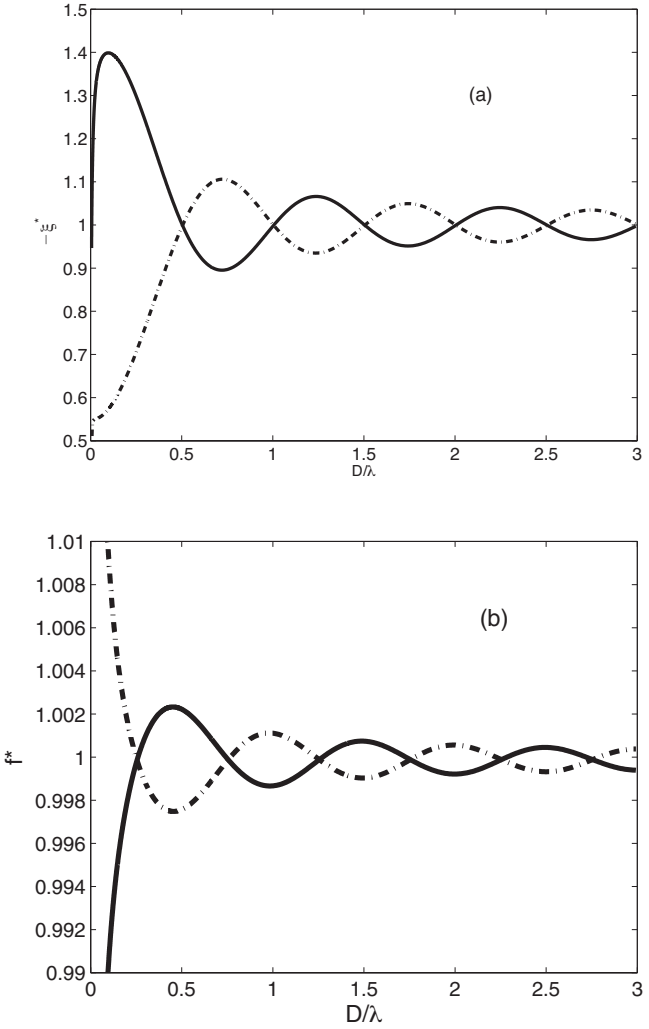

FIG. 3. Plot of $-\xi^*$ (a) and f^* (b) for the different modes predicted by the model with time delay. (—) $n=1$; (–·–) $n=2$. There are only two bubbles in the system and $R_0=2$ mm. Note the different y-axis scales.

$$\ddot{x}_2(t) + \omega_0\delta\dot{x}_2(t) + \omega_0^2 x_2(t) = -\frac{R_0}{D}\ddot{x}_1(t-\tau). \tag{22}$$

Both bubbles are of the same equilibrium radius R_0 separated by a distance D. The time delay is given by $\tau=D/c$. If we assume that τ is small, then using a Taylor series, the time delay term in Eq. (21) can be approximated as

$$\ddot{x}_2(t-\tau) \approx \ddot{x}_2(t) - \tau\dddot{x}_2(t). \tag{23}$$

Note that this approximation is only made for the purpose of the analysis in this section. Equation (23) is not used to obtain the results in Fig. 3. It is possible to obtain an expression for $\dddot{x}_2(t)$ by differentiating Eq. (22) as follows:

$$\dddot{x}_2(t) = -\omega_0\delta\ddot{x}_2(t) - \omega_0^2\dot{x}_2(t) - \frac{R_0}{D}\dddot{x}_1(t-\tau).$$

Substituting Eq. (23) into Eq. (21) gives

$$\ddot{x}_1(t) + \frac{R_0}{D}(1+\omega_0\delta\tau)\ddot{x}_2 + \omega_0\delta\dot{x}_1(t) + \frac{R_0}{D}\omega_0^2\tau\dot{x}_2(t) + \omega_0^2 x_1(t) + \left(\frac{R_0}{D}\right)^2\tau\dddot{x}_1(t-\tau) = 0. \tag{24}$$

Performing a similar exercise on the time delay term on the right hand side of Eq. (22) gives

$$\frac{R_0}{D}(1+\omega_0\delta\tau)\ddot{x}_1(t) + \ddot{x}_2 + \frac{R_0}{D}\omega_0^2\tau\dot{x}_1(t) + \omega_0\delta\dot{x}_2(t) + \omega_0^2 x_2(t) + \left(\frac{R_0}{D}\right)^2\tau\dddot{x}_2(t-\tau) = 0. \tag{25}$$

The coefficient of the last term of Eqs. (24) and (25), $(R_0/D)^2\tau$, is usually small so it is possible to ignore the (third derivative) time delay term on the right hand side of Eqs. (24) and (25). This will give us a coupled set of ordinary differential equations, which can be written in matrix form as

$$\begin{bmatrix} 1 & \frac{R_0}{D}(1+\omega_0\delta\tau) \\ \frac{R_0}{D}(1+\omega_0\delta\tau) & 1 \end{bmatrix}\begin{pmatrix}\ddot{x}_1(t)\\ \ddot{x}_2(t)\end{pmatrix} + \omega_0\delta\begin{bmatrix} 1 & \frac{R_0\omega_0}{D\delta}\tau \\ \frac{R_0\omega_0}{D\delta}\tau & 1 \end{bmatrix}\begin{pmatrix}\dot{x}_1(t)\\ \dot{x}_2(t)\end{pmatrix} + \begin{bmatrix}\omega_0^2 & 0\\ 0 & \omega_0^2\end{bmatrix}\begin{pmatrix}x_1(t)\\ x_2(t)\end{pmatrix} = \begin{pmatrix}0\\0\end{pmatrix}. \tag{26}$$

Equation (26) will result in a quadratic eigenvalue problem, which can be studied using conventional techniques (see Ref. 25). Since the damping is predominantly influenced by the matrix of the first derivative term, it is clear that the effects of time delay are to increase the overall damping of the system. This influence can be quantified by the parameter $R_0\omega_0\tau/D\delta$. Equation (26) also suggests that when the damping is small (i.e., when $\omega_0\delta \ll 1$), the effect of the time delay is more significant on the overall system's damping than on its frequency. Moreover, time delay apparently introduces an additional form of damping [see Eq. (26)] that is independent of the individual-bubble damping δ. A similar but more thorough exposition of this analysis can be found in the paper by Doinikov *et al.*[22]

It is possible to think of the physical effects of coupling with time delay as introducing an additional source of radiation "damping," which could either increase or decrease the net system damping. When time delay introduces a phase lag, the energy transferred to another bubble could be either more or less rapidly dissipated, depending on the location of the other bubble with respect to the phase of the traveling wave. The cyclical variation of the damping is also found by Feuillade[19] and a very similar explanation is given in that paper.

Kapodistrias and Dahl[33] carried out experimental measurements of the backscattering of sound from a two-bubble

system in water. Bubbles with a radius of 585 μm were used in their experiments and they were excited at frequencies between 80 and 140 kHz. The distances between the bubbles were varied between 1.2 and 70 mm and they reported that "for $D/\lambda \approx 1/2$, the backscattered radiation is maximized, while for $D/\lambda < 1/2$ the backscattered radiation is reduced considerably." This observation could be explained by considering the information in Fig. 3. While this figure was created for bubbles of 2 mm radii, a very similar graph can be generated for bubbles with radii 585 μm. If we assume that the symmetric mode is the dominant mode in the experiments, then Fig. 3 shows that when $D/\lambda \approx 1/2$ the damping is quite small compared to when $D/\lambda < 1/2$. This would lead to higher values of backscattered radiation for $D/\lambda \approx 1/2$ when compared to the data for $D/\lambda < 1/2$. Kapodistrias and Dahl[33] used a multiple scattering approach to explain this variation in scattered acoustic energy as a function of the ratio of the spacing of two bubbles to the sound wavelength. Here, we have shown that the self-consistent coupled-oscillator model with time delays can predict a similar dependence on the bubble spacing to wavelength ratio in a multiple bubble system.

Natural frequencies and damping plots for the situation for ten bubbles ($N=10$) are shown in Figs. 4 (no time delay) and 5 (with time delays). Similar to the two-bubble ($N=2$) case, Fig. 4 shows that the curves for damping and natural frequencies for the model without time delays do not cross over. This indicates that the natural frequencies and damping corresponding to the $n=1$ mode will always be smaller than the damping and natural frequencies for the higher modes. This situation seems to be independent of the separation D of the bubbles in the chain. When time delays are taken into account, Fig. 5 shows that similarly to the $N=2$ case, the curves for the ξ^* cross over at $D/\lambda=(k+1)/2$ and the curves for f^* cross over when $D/\lambda=(2k+1)/4$ where $k=0,1,2,\ldots$. Similar to the two-bubble case, the results here for the time delay model can be explained when the incident wave emanated from the neighboring bubble is assumed to be a traveling wave. The ξ^* plots of the time delay model for the $N=2$ and $N=10$ cases [Figs. 3(a) and 5(a)] show that the maximum and minimum damping values occur because the phase of the incident wave is changed, i.e., depending on its phase, the incident wave can suppress or increase the oscillation mode of the bubble.

One way of analyzing the effects of time delay on the system is to plot the ratios of the natural frequencies,

$$\alpha = f_{\text{time delay}}/f_{\text{no time delay}}, \tag{27}$$

and damping

$$\beta = \xi_{\text{time delay}}/\xi_{\text{no time delay}}, \tag{28}$$

for both models at particular values of D/λ. Plots of α for $N=2$ and $N=10$ are shown in Fig. 6 and similar plots for β are shown in Fig. 7. It is clear that adding time delays do not have much effect on the natural frequencies of the system. The maximum variation for the $N=2$ chain is only about 0.5% and the $N=10$ chain has a maximum variation of less than 3%. Thus, there are only very small variations in the natural frequencies even when there are more bubbles in the chain. It is also clear that, in general, adding time delays increases the natural frequency of the lowest ($n=1$) mode but decreases the frequency of the highest ($n=N$) mode. In terms of damping, Fig. 7 shows that time delays have a dramatic effect on the damping of the individual modes. For $N=2$, there is almost a 40% increase in damping for the $n=1$ mode for small values of D/λ. The $n=2$ mode damping decreases by about 45% when time delays are taken into account. When N is increased to 10, Fig. 7(b) shows that the effects of time delays are even larger. The reason why time delay has a greater effect on system damping than on the natural frequencies is explained with Eq. (26) and the corresponding discussion on page 16.

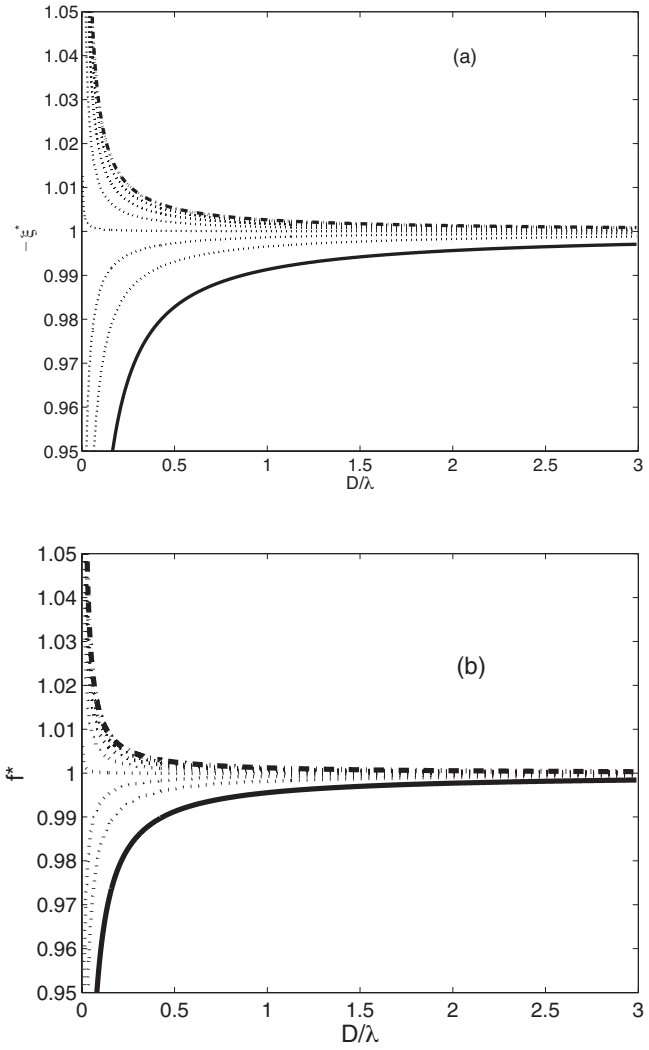

FIG. 4. Plot of $-\xi^*$ (a) and f^* (b) for the different modes predicted by the model without time delay. (—) $n=1$; (– –) $n=10$; (···) all intermediate modes. The analyzed system consists of an equally spaced bubble chain consisting of ten bubbles with equilibrium radii, $R_0=2$ mm.

B. Comparison with experimental data

In order to assess the importance of time delays, predicted data from the theoretical models will be compared with experimental data from Nikolovska *et al.*,[21] who carried out a high-spatial resolution experimental investigation on the evolution of the acoustic energy along the bubble chain. The experimental principles can be found in Ref. 20 and full

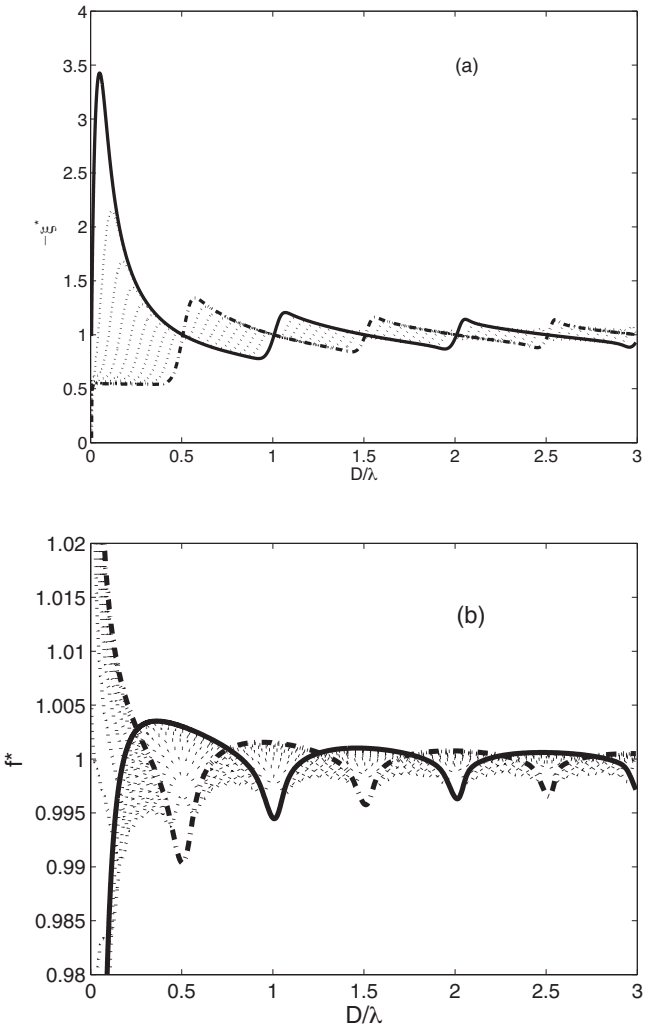

FIG. 5. Plot of $-\xi^*$ (a) and f^* (b) for the different modes predicted by the model with time delay. (—) $n=1$; (–·–) $n=10$; (···) all intermediate modes. The analyzed system consists of an equally spaced bubble chain consisting of ten bubbles with equilibrium radii, $R_0=2$ mm. Note the different y-axis scales.

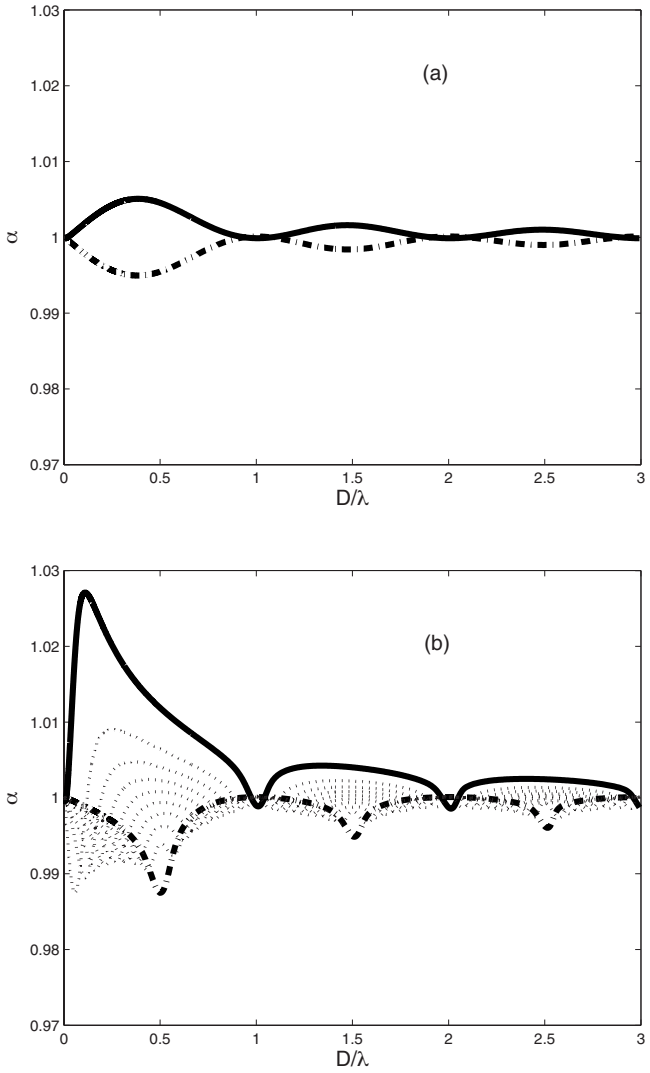

FIG. 6. Ratio of the natural frequencies, α, for $N=2$ (a) and $N=10$ (b). (—) $n=1$; (–·–) $n=N$; (···) all intermediate modes. The analyzed system consists of an equally spaced bubble chain consisting of bubbles with equilibrium radius, $R_0=2$ mm.

details of the high-resolution experiments can be found in Ref. 21. Air bubbles were introduced into a tank with a 1 mm radius nozzle. Depending on the bubble production rate (BPR), the bubbles generated from this nozzle had radii between 1 and 2.35 mm (see Table I). Photographic images similar to that shown in Fig. 1 were used to determine the size of the bubbles. The comparison with theoretical predictions will be made along a vertical line, which is 6 cm from the nozzle. Hydrophones were used to record data at 30 kHz. The total period of data acquisition, T, was $1024/30\,000 = 0.0341$ s ≈ 34 ms. The distance between bubbles in the chain ranged from 36 mm at the lowest BPR to 6.5 mm at the highest BPR. In this system, most of the acoustic energy is generated when the bottom bubble detaches from the nozzle. In an earlier study, Manasseh *et al.*[20] showed that there is an anisotropic distribution of acoustic energy in the vicinity of the bubble chain. Experimental data show that the rms value of pressure dies off much faster as we move away from the chain than along the bubble chain, indicating that the transfer of acoustic energy is more efficient along the bubble chain.

Instantaneous snapshots from the experimental data of the acoustic pressure profile are shown in Fig. 8 at time instances $t/T_0=7.2$, 7.6, 7.9, and 8.3, where T_0 is the Minnaert period of a single isolated bubble. It is clear that there is a preference for the propagation of acoustic energy along the bubble chain. In order to compute the propagation speed along the bubble chain, V_p, a numerical algorithm was developed to detect and track the local maximum of the pressure profile (peak pressure) measured from the experimental data. The location of the local pressure maxima found by the algorithm is indicated by ∘ in Fig. 8. By following these ∘ symbols, it is possible to calculate V_p. When the peak of the acoustic pressure wave leaves the domain, the algorithm would detect and follow another peak from the bottom of the bubble chain.

The results are shown in Fig. 9. The vertical axis is the location of the peak pressure along the bubble chain and the horizontal axis shows the corresponding value of V_p normalized by the speed of sound in water, c. Only data from the 20 Hz BPR case are shown. Data from all other cases show

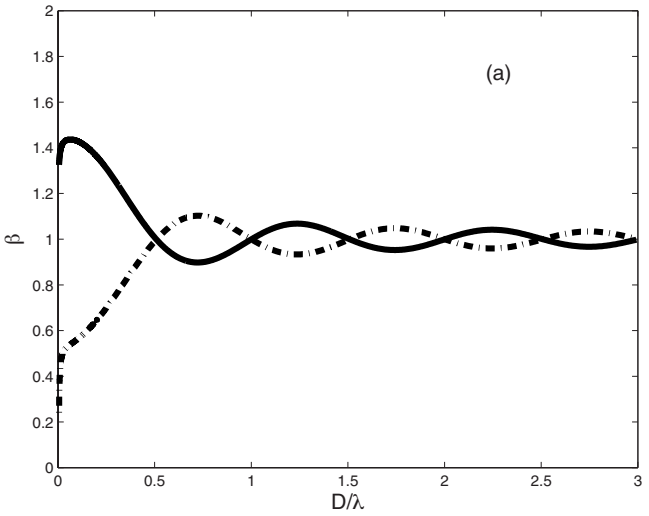

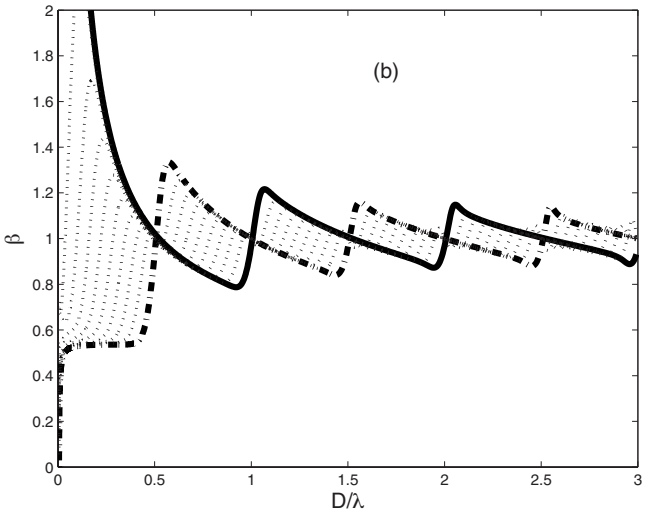

FIG. 7. Ratio of the damping, β, for $N=2$ (a) and $N=10$ (b). (—) $n=1$; (–·–) $n=N$; (···) all intermediate modes. The analyzed system consists of an equally spaced bubble chain consisting of bubbles with equilibrium radius, $R_0=2$ mm.

similar trends. Postprocessing of the experimental data shows that V_p is smaller at the bottom of the bubble chain and increases slightly further up the bubble chain [see Fig. 9(a)]. In general, V_p calculated from the experimental data is usually smaller than c. However, there are a small number of instances where V_p calculated from the experimental data exceeds c, which is due to the noise in the experimental data. Data from predictions using the coupled-oscillator model without time delays are shown in Fig. 9(b). There are large variations in V_p as the acoustic pressure moves up the bubble chain. When the pressure peak is at the bottom of the chain, predicted values of V_p are usually smaller than c. As the pressure peak moves up the chain, predicted values of V_p increase to nearly $3c$. This is unrealistic and can be explained by recalling that Eq. (2) assumes that any disturbance from a neighboring bubble immediately affects (travels at an infinite speed to) a nearby bubble. Thus, it is unsurprising that coupling these equations without time delays will produce an estimate of V_p, which is much larger than c. This anomaly is overcome by incorporating time delays into the coupled-oscillator model, as shown in Fig. 9(c). The predicted values of V_p are much more reasonable, closer to the values of V_p calculated from experimental data [compare Fig. 9(a) with Fig. 9(c)]. The coupled-oscillator model with time delays also predicts a smaller variation of V_p as the pressure peak moves up the bubble chain, again consistent with V_p calculated using experimental data.

TABLE I. Parameters from experimental studies. Data are from the 1 mm nozzle.

BPR (Hz)	Frequency (kHz)	Radius (mm)	D (mm)	N
10	1.97	1.18	36	40
12	1.90	1.35	32.8	48
14	1.88	1.41	30.0	56
18	1.8	1.50	26.6	72
20	1.79	1.52	19.7	80
22	1.68	1.55	17.0	88
24	1.52	1.64	16.0	96
26	1.21	1.70	14.0	104
29	1.15	1.88	10.3	116
31	1.06	2.00	9.2	124
34	0.91	2.10	7.5	136
38	0.84	2.35	6.5	152

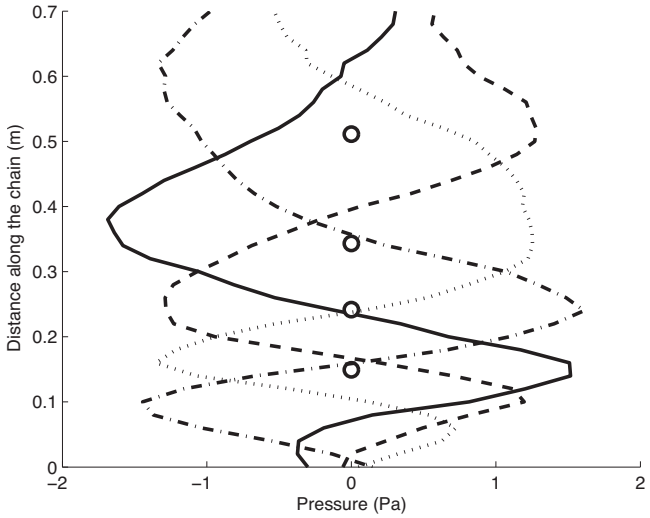

FIG. 8. Vertical profiles of instantaneous pressure at $t/T_0=7.2$ (—), 7.6 (–·–), 7.9 (···), 8.3 (----). The ○ in the figure marks the positions of the numerically predicted local pressure maxima.

From the experimental and numerical data, an observation that it was not possible to follow the pressure peak throughout the domain for $t/T_0<5$ and $t/T>1/4$ where $T=1024/30\,000=0.034$ s=34 ms is the total time period of data acquisition in the experiments was made. Usually, $t/T>1/4$ would correspond to approximately $t/T_0>20$. For $t/T_0<5$, the peak of the the acoustic pressure profile flattens out as it reaches the top of the domain, which makes the maximum difficult to detect numerically. On the other hand, for $t/T>1/4$, the signal decays to essentially zero, thus any local peak in the data would be almost undetectable. So it is only possible to calculate the average values of V_p for $T_0/5<t<(1/4)T$ and the results are shown in Fig. 10. At a smaller BPR, there are large discrepancies between the

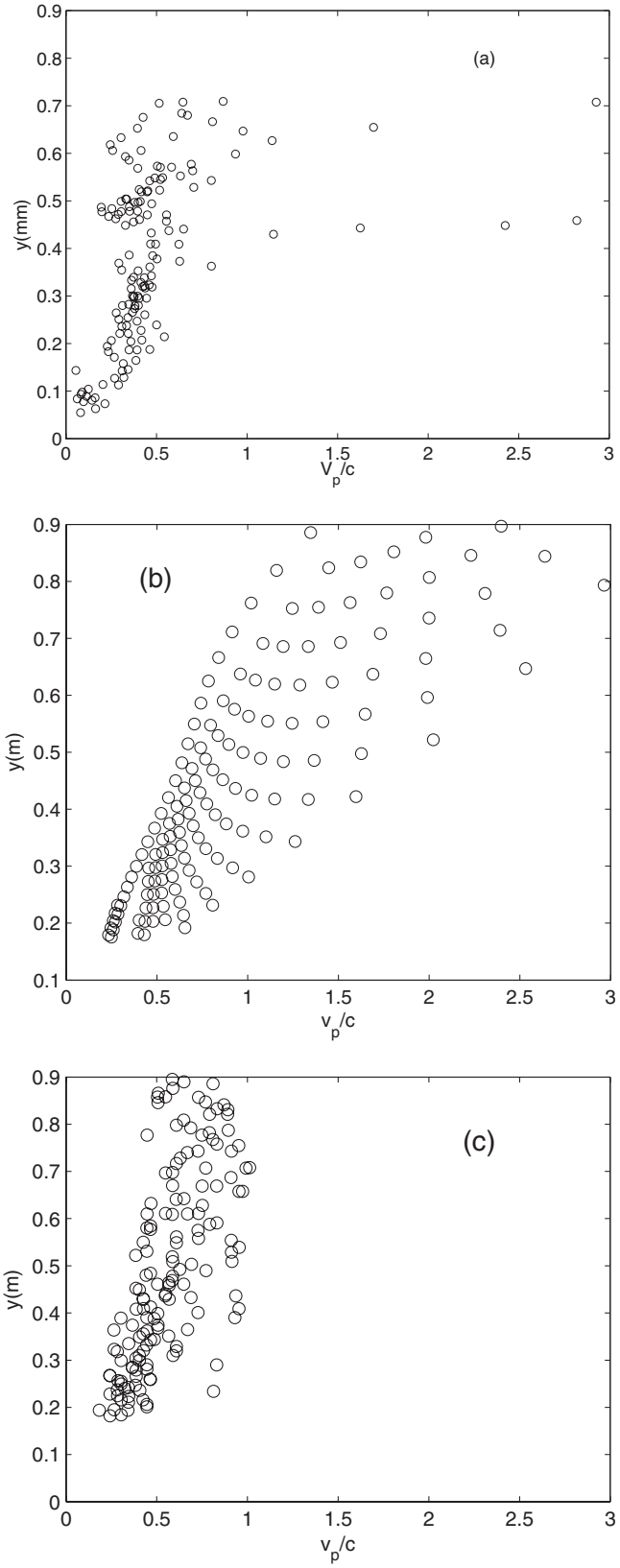

FIG. 9. Comparing the predicted phase velocity V_p/c of the different models with experimental data at BPR=20 Hz. (a) is the experimental data, (b) model without time delays, and (c) model with time delays.

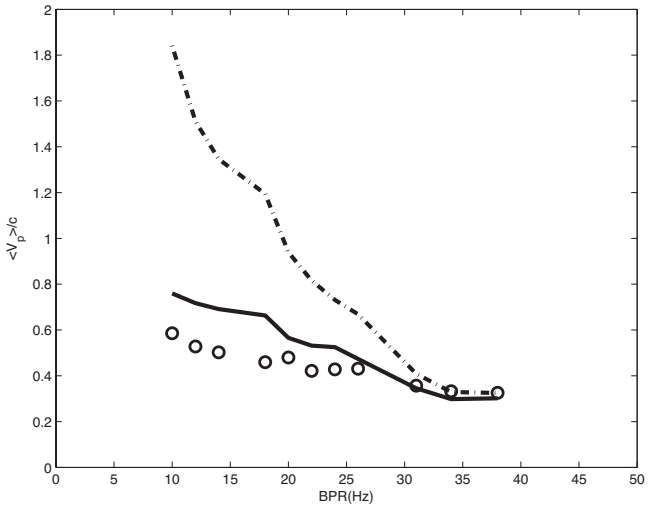

FIG. 10. Comparing the average phase velocity $\langle V_p \rangle$, normalized by the speed of sound in water c for experimental data at different bubble production rates (BPRs). (○) Experimental data; (–·–) numerical model with no time delays; (—) numerical model with time delays.

model without time delay and the model with time delay. As noted above, there is better agreement between the experimental data and the mathematical model when time delays are taken into account. As we increase the BPR, there are more bubbles in the chain and the distance between bubbles in the chain becomes smaller. Hence, the effects of time delays are reduced. This is one possible reason why Fig. 10 shows that there is good agreement with experimental data for both models at a large BPR.

The eigenvalue results (Fig. 7) had showed that time delays had an increasing effect on the damping for larger values of N. However, Fig. 9 shows time delays had a decreasing effect on the propagation speed as N (BPR) increased. This is probably because different physical phenomena are responsible for overall system damping and propagation speed. As N increases, the energy transfer to all other bubbles (affecting overall dissipation) is enhanced because the coupling becomes stronger as bubbles become closer. This increases the relevance of time delays, which provide a mechanism for altered dissipation as explained on page 18. However, as N increases, the lag in information transfer to neighboring bubbles (affecting propagation speed) is decreased. This reduces the relevance of time delays.

From Fig. 10, the time delay model produces a better comparison on propagation speeds of the non-time-delay model, particularly when bubbles are far apart (low BPR). In contrast, the comparison between experimental and numerical data for the distribution of rms pressure, P_{rms} (Fig. 11), does not suggest a clear superiority of one model over another. In calculating P_{rms} for Fig. 11, the averaging is done over $0<t<T$. Only data from four BPRs are shown but data from all other BPRs show the same trends. Farther from the bubble generation point (i.e., at larger y), the time delay model generates pressures that are closer to the experimental data than the non-time-delay model. Pressures in the time delay model are lower than in the non-time-delay model, mainly due to the higher damping of the modes when time delays are taken into account [compare data in Figs. 4(a) and 5(a)]. As the acoustic wave travels up the bubble chain, the incorporation of time delays produces an enhanced damping effect on the wave, which reduces the predicted values of

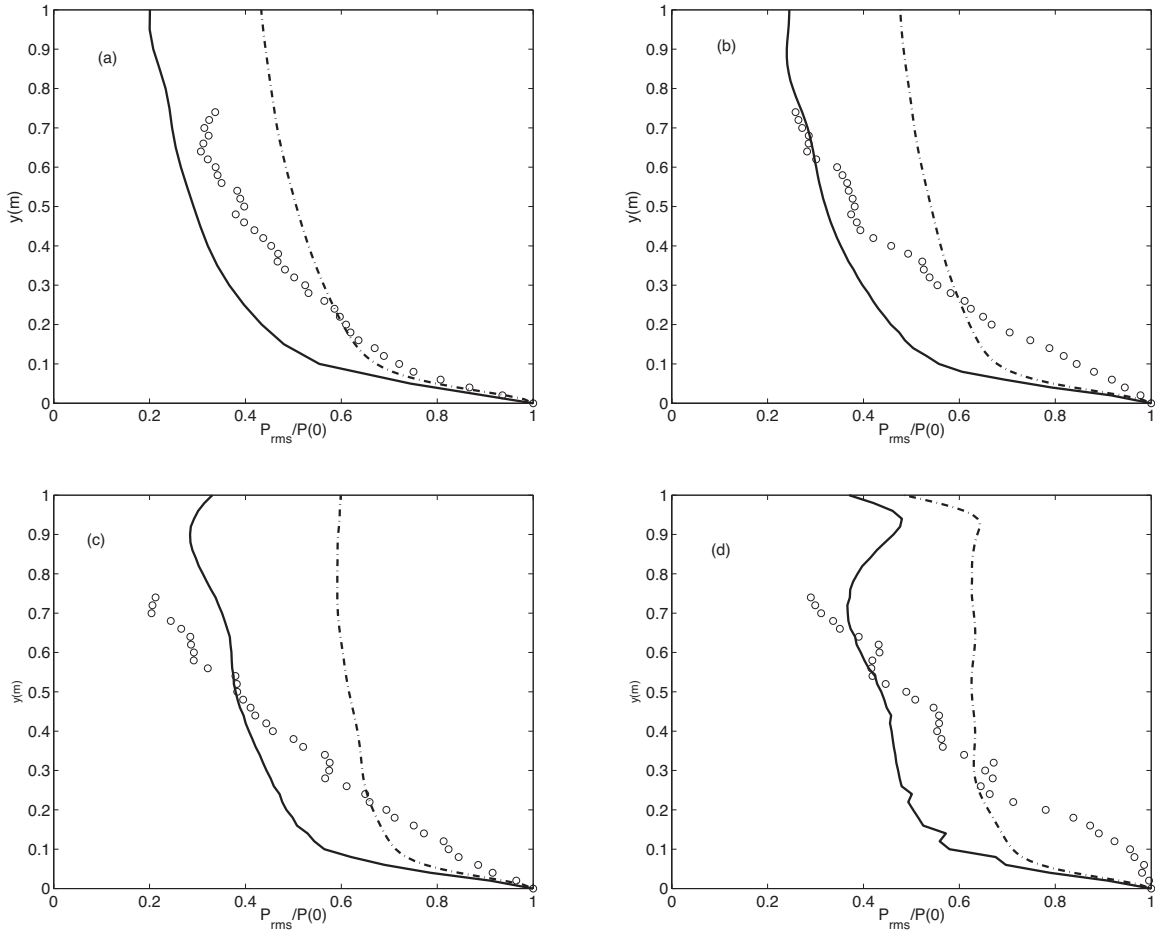

FIG. 11. Comparison of the rms pressure for different bubble production rates (BPRs). (a) BPR=22 Hz, (b) BPR=26 Hz, (c) BPR=31 Hz, and (d) BPR =38 Hz. (○) Experimental data; (—) predictions using the model with time delays; (–·–) predictions using numerical model without time delay.

P_{rms} further up the bubble chain. However, the trends, in general, do not match the experimental data, particularly at a higher BPR.

The discrepancies between the experimental data and theoretical models could be due to a number of factors. Clearly, the shape of the bubbles is not constant (Fig. 1), and this is known to "detune" the resonant frequency ω_0.[34] The spacing between the bubbles is also not a constant but varies as the bubble transitions from its initial vertical trajectory to a spiral trajectory.[35,36] Perhaps the most significant issue is that both theoretical models assume that the ratio R_0/D is very small (see discussion on page 6). In the experiments, R_0/D ranges from about 0.09 to approximately 0.36. These values are not very small, and the approximation worsens for a high BPR, consistent with the worsening of the comparison with experiment at a high BPR.

IV. CONCLUSIONS

An investigation on the effects of time delays in the coupled-oscillator model has been carried out. The models have been applied to the case of a bubble chain and results from the analysis show that the main effects of time delays are to increase the amount damping of the lowest mode and decrease the amount of damping in the highest mode. If there are no time delays, the lowest frequency mode has the smallest amount of damping. When time delays are taken into account, the situation is reversed with the highest damping occurring at the lowest frequency. This study also shows that time delays do not have a significant effect on the natural frequencies of each mode. However, the addition of time delays can have a major impact on the damping of each individual eigenmode.

Previous investigations have shown that there is a preference for acoustic energy to propagate along a bubble chain. It has also been reported that the average speed of propogation of acoustic energy is much smaller than the speed of sound in water. Calculations conducted without taking time delay into consideration show propagation speeds much faster than the speed of sound in water. Time delays reduce the speed of propagation and predict propagation speeds much closer to experimental data.

ACKNOWLEDGMENT

We would like to thank. A. Doinikov, from Byelorussian State University, Belarus, for introducing us to the idea of time delay and many fruitful discussions.

[1]T. Leighton, *The Acoustic Bubble* (Academic, London, 1994).
[2]E. A. Zabolotskaya, "Interaction of gas bubbles in a sound field," Sov. Phys. Acoust. **30**, 365–368 (1984).
[3]I. Tolstoy, "Superresonant systems of scatterers," J. Acoust. Soc. Am. **80**, 282–294 (1986).
[4]H. Ogũz and A. Prosperetti, "A generalization of the impulse and virial

theorems with an application to bubble oscillations," J. Fluid Mech. **218**, 143–162 (1990).
[5]A. A. Doinikov and S. T. Zavtrak, "On the mutual interaction of two gas bubbles in a sound field," Phys. Fluids **7**, 1923–1930 (1995).
[6]C. Feuillade, "Acoustically coupled gas bubbles in fluids: Time-domain phenomena," J. Acoust. Soc. Am. **109**, 2606–2615 (2001).
[7]P.-Y. Hsaio, M. Devaud, and J.-C. Bacri, "Acoustic coupling between two air bubbles in water," Eur. Phys. J. D **4**, 5–10 (2001).
[8]M. Ida, "A characteristic frequency of two mutually interacting gas bubbles in an acoustic field," Phys. Lett. A **297**, 210–217 (2002).
[9]M. Ida, "Number of transition frequencies of a system containing an arbitrary number of gas bubbles," J. Phys. Soc. Jpn. **71**, 1214–1217 (2002).
[10]M. Ida, "Avoided crossings in three coupled oscillators as a model system of acoustic bubbles," Phys. Rev. E **72**, 036306 (2005).
[11]K. W. Commander and A. Prosperetti, "Linear pressure waves in bubbly liquids: Comparison between theory and experiments," J. Acoust. Soc. Am. **85**, 732–746 (1989).
[12]R. Duraiswami, S. Prabhukumar, and G. L. Chahine, "Bubble counting using an inverse scattering method," J. Acoust. Soc. Am. **104**, 2699–2717 (1998).
[13]M. Nicholas, R. A. Roy, L. A. Crum, H. N. Ogũz, and A. Prosperetti, "Sound emission by a laboratory bubble cloud," J. Acoust. Soc. Am. **95**, 3171–3182 (1994).
[14]A. D. Phelps, D. G. Ramble, and T. G. Leighton, "The use of a combination frequency technique to measure the surf zone bubble population," J. Acoust. Soc. Am. **101**, 1981–1989 (1996).
[15]E. J. Terrill and K. W. Melville, "A broadband acoustic technique for measuring bubble size distributions: laboratory and shallow water measurements," J. Atmos. Ocean. Technol. **17**, 220–239 (2000).
[16]A. B. Pandit, J. J. Varley, R. B. Thorpe, and J. F. Davidson, "Measurement of bubble size distribution: An acoustic technique," Chem. Eng. Sci. **47**, 1079–1089 (1992).
[17]J. W. R. Boyd and J. Varley, "The uses of passive measurement of acoustic emissions from chemical engineering processes," Chem. Eng. Sci. **56**, 1749–1767 (2001).
[18]R. Manasseh, R. F. LaFontaine, J. Davy, I. C. Shepherd, and Y. Zhu, "Passive acoustic bubble sizing in sparged systems," Exp. Fluids **30**, 672–682 (2001).
[19]C. Feuillade, "Scattering from collective modes of air bubbles in water and the physical mechanism of superresonances," J. Acoust. Soc. Am. **117**, 1178–1190 (1995).
[20]R. Manasseh, A. Nikolovska, A. Ooi, and S. Yoshida, "Anisotropy in the sound field generated by a bubble chain," J. Sound Vib. **278**, 807–823 (2004).
[21]A. Nikolovska, R. Manasseh, and A. Ooi, "On the propagation of acoustic energy in the vicinity of a bubble chain," J. Sound Vib. **306**, 507–523 (2007).
[22]A. Doinikov, R. Manasseh, and A. Ooi, "Time delays in coupled multiple bubble systems," J. Acoust. Soc. Am. **117**, 47–50 (2005).
[23]V. Twersky, "Multiple scattering of waves and optical phenomena," J. Opt. Soc. Am. **52**, 145–171 (1962).
[24]C. Clay and H. Medwin, *Acoustical Oceanography* (Wiley, New York, 1977).
[25]F. Tisseur and K. Meerbergen, "The quadratic eigenvalue problem," SIAM Rev. **43**, 235–286 (2001).
[26]H. Hu, E. Dowell, and L. Virgin, "Stability estimation of high dimensional vibrating systems under state delay feedback control," J. Sound Vib. **214**, 497–511 (1998).
[27]M. Longuet-Higgins, B. Kerman, and K. Lunde, "The release of air bubbles from an underwater nozzle," J. Fluid Mech. **230**, 365–390 (1991).
[28]A. Prosperetti and H. Ogũz, "The impact of drops on liquid surfaces and the underwater noise of rain," Annu. Rev. Fluid Mech. **25**, 577–602 (1993).
[29]H. C. Pumphrey and P. A. Elmore, "The entrainment of bubbles by drop impacts," J. Fluid Mech. **220**, 539–567 (1990).
[30]Y. Y. Hu and B. C. Khoo, "An interface interaction method for compressible multifluids," J. Comput. Phys. **198**, 35–64 (2004).
[31]A. Bui and R. Manasseh, in A CFD Study of the Bubble Deformation During Detachment, Fifth International Conference on CFD in the Process Industries, Melbourne, Australia, 13–15 December (2006).
[32]E. Payne, S. Illesinghe, A. Ooi, and R. Manasseh, "On the resonances of bubbles attached to a rigid boundary," J. Acoust. Soc. Am. **118**, 2841–2849 (2005).
[33]G. Kapodistrias and P. Dahl, "Effects of interaction between two bubble scatterers," J. Acoust. Soc. Am. **107**, 3006–3017 (2000).
[34]M. Strasberg, "The pulsation frequency of nonspherical gas bubbles in liquid," J. Acoust. Soc. Am. **25**, 536–537 (1953).
[35]R. Clift, J. R. Grace, and M. E. Weber, *Bubbles, Drops and Particles* (Academic, London, 1978).
[36]S. Yoshida, R. Manasseh, and N. Kajio, in The Structure of Bubble Trajectories Under Continuous Sparging Conditions, Third International Conference on Multiphase Flow, Lyon, France (1998), Vol. **426**, pp. 1–8.